NeuroImage 247 (2022) 118742

Contents lists available at ScienceDirect

NeuroImage

journal homepage: www.elsevier.com/locate/neuroimage

Descending pain modulatory efficiency in healthy subjects is related to structure and resting connectivity of brain regions

Vincent Huynh[a,b,*], Robin Lütolf[b], Jan Rosner[b,c], Roger Luechinger[d], Armin Curt[b], Spyros Kollias[a], Lars Michels[a], Michèle Hubli[b]

[a] Department of Neuroradiology, Clinical Neuroscience Center, University Hospital Zurich & University of Zurich, Zurich, Switzerland
[b] Spinal Cord Injury Center, Balgrist University Hospital, University of Zurich, Forchstrasse 340, Zurich 8008, Switzerland
[c] Department of Neurology, University Hospital Bern, Inselspital, University of Bern, Bern, Switzerland
[d] Institute for Biomedical Engineering, University and ETH Zurich, Zurich, Switzerland

ARTICLE INFO

Keywords:
Endogenous pain modulation
Conditioned pain modulation
Magnetic resonance imaging
Voxel-based morphometry
Resting-state functional connectivity

ABSTRACT

The descending pain modulatory system in humans is commonly investigated using conditioned pain modulation (CPM). Whilst variability in CPM efficiency, i.e., inhibition and facilitation, is normal in healthy subjects, exploring the inter-relationship between brain structure, resting-state functional connectivity (rsFC) and CPM readouts will provide greater insight into the underlying CPM efficiency seen in healthy individuals. Thus, this study combined CPM testing, voxel-based morphometry (VBM) and rsFC to identify the neural correlates of CPM in a cohort of healthy subjects (n =40), displaying pain inhibition (n = 29), facilitation (n = 10) and no CPM effect (n = 1). Clusters identified in the VBM analysis were implemented in the rsFC analysis alongside key constituents of the endogenous pain modulatory system. Greater pain inhibition was related to higher volume of left frontal cortices and stronger rsFC between the motor cortex and periaqueductal grey. Conversely, weaker pain inhibition was related to higher volume of the right frontal cortex - coupled with stronger rsFC to the primary somatosensory cortex, and rsFC between the amygdala and posterior insula. Overall, healthy subjects showed higher volume and stronger rsFC of brain regions involved with descending modulation, while the lateral and medial pain systems were related to greater pain inhibition and facilitation during CPM, respectively. These findings reveal structural alignments and functional interactions between supraspinal areas involved in CPM efficiency. Ultimately understanding these underlying variations and how they may become affected in chronic pain conditions, will advance a more targeted subgrouping in pain patients for future cross-sectional studies investigating endogenous pain modulation.

1. Introduction

The descending pain modulatory system in humans is commonly investigated by the psychophysical paradigm of conditioned pain modulation (CPM). CPM paradigms involve the application of a noxious test stimulus (TS) which becomes modulated by another heterotopic noxious conditioning stimulus (CS) (Nir and Yarnitsky, 2015; Yarnitsky et al., 2015). The evaluation of the pain perceived by the TS is performed before, and either during or after CS application (Kennedy et al., 2016). CPM efficiency, i.e. inhibition and facilitation of the TS, may be influenced by factors such as sex (Granot et al., 2008), age (Edwards et al., 2003), expectation (Bjørkedal and Flaten, 2012), and experimental design (Fernandes et al., 2019). A lack of pain inhibition during CPM is more frequently observed in individuals who develop post-operative pain (Yarnitsky et al., 2008; Vaegter et al., 2017) and individuals suffering from chronic pain conditions, e.g. neuropathic pain after spinal cord injury (Albu et al., 2015; Gruener et al., 2016), fibromyalgia (O'Brien et al., 2018) and low back pain (McPhee et al., 2019). These studies suggest that the assessment of CPM could be predictive of post-operative pain, and underlying differences of the descending pain modulatory system may contribute to the development of chronic pain.

Although the typical inhibitory effects during CPM are assumed to be mediated by a spino-bulbo-spinal loop, i.e. ventrolateral periaqueductal grey (vlPAG), rostroventral medulla (Le Bars et al., 1979a,1979b; Dickenson et al., 1980; Le Bars et al., 1981, 1992; Villanueva and Le Bars, 1995), accumulating evidence suggests that additional cerebral regions are associated with CPM efficiency. Studies have observed relationships between CPM efficiency and resting-state functional connectivity (rsFC) of pain modulatory landmarks, e.g. anterior cingulate cortex (ACC) and prefrontal regions (Harper et al., 2018; Argaman et al.,

* Corresponding author at: Spinal Cord Injury Center, Balgrist University Hospital, University of Zurich, Forchstrasse 340, Zurich 8008, Switzerland.
E-mail address: vincent.huynh@balgrist.ch (V. Huynh).

https://doi.org/10.1016/j.neuroimage.2021.118742.
Received 12 August 2021; Received in revised form 26 October 2021; Accepted 16 November 2021
Available online 1 December 2021.

2020). Healthy subjects with greater pain inhibition showed stronger rsFC between the vlPAG and pons (Harper et al., 2018) and between the prefrontal regions, posterior cingulate and ACC (Argaman et al., 2020). Conversely, healthy subjects displaying pain facilitation had reduced rsFC in the same regions (Harper et al., 2018). Furthermore, animal studies have observed an influence of direct cortical-spinal pathways, i.e. ACC (Chen et al., 2018), primary motor (M1) (Lopes et al., 2019) and somatosensory cortices 1 (S1) (Liu et al., 2018), and indirect cortical-to-spinal pathways, i.e. amygdala-prefrontal-PAG (Huang et al., 2019) on pain modulation. Structural brain differences are also associated with CPM efficiency. Weaker pain inhibition was associated with greater cortical thickness of the orbitofrontal cortex in healthy subjects (Piché et al., 2013) and reduced white matter of the precuneus in chronic neck pain sufferers (Coppieters et al., 2018). These studies highlight that structure and rsFC of brain regions are related to variability in descending pain modulation and may be altered in chronic pain. However, the inter-relationship between brain structure, rsFC and CPM efficiency in healthy subjects remains unexplored and determining this relationship will provide further insight into the variability of descending pain modulation, especially in those not expressing pain inhibition.

Therefore, this study explores the neural correlates of endogenous pain modulation in healthy subjects. We investigated the brain correlates of CPM efficiency in our entire cohort using voxel-based morphometry (VBM) analyses and rsFC with a seed-to-voxel approach. Specifically, we explored the rsFC in regions showing grey matter volume (GMV) associations with CPM efficiency and areas commonly involved with descending pain modulation, e.g. vlPAG, ACC and amygdala (Ossipov et al., 2010). Based on prior studies, we hypothesised that weaker pain inhibition is associated with higher amounts of GMV in the frontal cortices, whilst greater pain inhibition is related to stronger rsFC in pain modulatory regions, e.g. vlPAG. Overall, individual variability of CPM effect will impact the relationship between structural and functional correlates.

2. Material and methods

2.1. Subjects

Forty-two healthy subjects were recruited for this study. These individuals were contacted and recruited with online flyer advertisements at the University Hospital Zurich and Balgrist University Hospital, Switzerland. The inclusion criteria were: i) ages between 18 and 80 years old, ii) no history of neurological or psychological conditions, iii) no previous history of chronic pain or pain during participation and iv) not taking any psychoactive medication. All subjects provided written informed consent prior to all assessments and were reimbursed for their participation. All procedures described below were in accordance with the Declaration of Helsinki. The study has been approved by the local ethics board 'Kantonale Ethikkommission Zürich, KEK' (EK-04/2006, PB_2016–02,051, clinicaltrial.gov number: NCT02138344).

2.2. Study design

Prior to neuroimaging and CPM, subjects completed two questionnaires: the Pain Catastrophizing Scale (PCS) (Sullivan et al., 1995) and Beck Depression Inventory version II (BDI-II) (Dozois et al., 1998). In order to test for sensory integrity in the tested area, thermal thresholds were assessed according to the quantitative sensory testing protocol of the German Research Network on Neuropathic Pain (Rolke et al., 2006). Warm detection and heat pain thresholds (WDT and HPT, respectively) measurements were performed with the PATHWAY Pain & Sensory Evaluation system (Medoc Ltd, Ramat Yishai, Israel) using a 3 cm x 3 cm square thermode attached at the volar forearm. Subjects were blinded from the operator screen during the measurement. Thermal thresholds were determined by averaging three trials of individual stimuli. Safety temperatures for WDT and HPT were set at 55 °C. After obtaining thermal thresholds, subjects who understood the instructions clearly were familiarised with one TS and were acquainted with the instructions of MRI acquisition and CPM procedure including the pain rating process.

2.3. Conditioned pain modulation

A parallel CPM paradigm with two conditions was performed in the MRI scanner: i) TS with a CS (TS-CPM) and ii) TS with a sham condition (TS-Sham). Each condition was randomised per subject and lasted 6:10mins. A five-minute break was placed between each condition. The CS consisted of two ice bags covering the non-dominant hand for the whole duration of the condition. Each of the ice bags contained ~600 g of ice and 250 ml of water guaranteeing a stable temperature of around 0 °C. Pain rating of the CS from pilot data (n = 5) indicated it being an appropriate noxious stimulus with an averaged reported pain of 7.0 (range= 6.3–8.0) on a numeric rating scale (NRS, 0 being "no pain" and 10 "worst pain imaginable"). An appropriate noxious stimulus is determined at an intensity of 4/10 as recommended by Yarnitsky et al. (2015). For the sham condition, the two bags with water at skin temperature (~32 °C) were used and provided a non-noxious stimulus. The TS was performed with the same 3 cm x 3 cm square thermode (Medoc Ltd, Ramat Yishai, Israel) attached on the volar forearm of the dominant hand. The position of the thermode was slightly shifted between the conditions (TS-CPM, TS-Sham) to avert sensitisation effects. Each TS had a fixed target temperature of 47.5 °C and lasted a total of 10 s including ramp time (~2.5 s ramp up (6.2 °C/s), 5-s plateau, ~2.5 s ramp down (6.2 °C/s)). Eight TS were performed with an inter-stimulus interval of 35 s per condition. Following each TS, subjects had a total of 20 s to rate their perceived pain of the TS and CS (10 s each) on a NRS projected on the NordicNeuroLab 32″ screen (NordicNeuroLab, Norway and USA, https://www.nordicneurolab.com) using a manual response unit placed in their dominant hand. The manual response unit was programmed to either move a cursor up or down the NRS per click of the allocated button, i.e. if subjects perceived the pain of the TS to be a "five" subjects clicked button 1 five times to move the cursor up the NRS. Subjects were always prompted to rate the TS followed by rating of the CS. Fig. 1 summarizes the CPM paradigm including the TS procedure. This CPM paradigm was adapted from a previous study utilising similar ice bags, noxious stimuli and block timings (Sprenger et al., 2011).

2.4. MRI data acquisition

All subjects' images were obtained using a 3.0 Tesla Philips Ingenia system (Philips Medical Systems, Best, the Netherlands) using a 32-channel Philips head coil. Structural and resting-state functional MRI data acquisition was performed prior to the CPM paradigm. 3D T1-weighted (T1w) structural images were acquired with a Turbo Field Echo sequence with the following parameters: repetition time (TR), 8.1 ms; echo time (TE), 3.7 ms; flip angle (FA), 8°; number of slices, 160; slice thickness, 1 mm; field of view (FOV), 240 × 240 × 160mm^3; matrix, 240 × 240 and isotropic voxel 1 × 1 × 1 mm^3 and a scan time of 4:53 mins. Resting-state functional images were acquired using an echo-planar-imaging sequence with the following parameters: TR, 2000 ms; TE, 30 ms; FA, 78°; number of slices, 36; FOV, 220 × 136 × 220mm^3; matrix, 72 × 74; voxel size, 3.0 × 3.0 × 3.0 mm; reconstructed voxel size, 1.72 × 1.72 × 3 mm^3 and a scan time of 5:00 mins. During this time, subjects were instructed to relax, remain awake with eyes fixating on a motionless cross, projected on a NordicNeuroLab 32″ screen (NordicNeuroLab, Norway and USA, https://www.nordicneurolab.com). To minimise head motion, cushions were placed around the subject's head. Next to structural and resting-state functional MRI data, task-related functional MRI data was acquired during the CPM paradigm and will be reported separately.

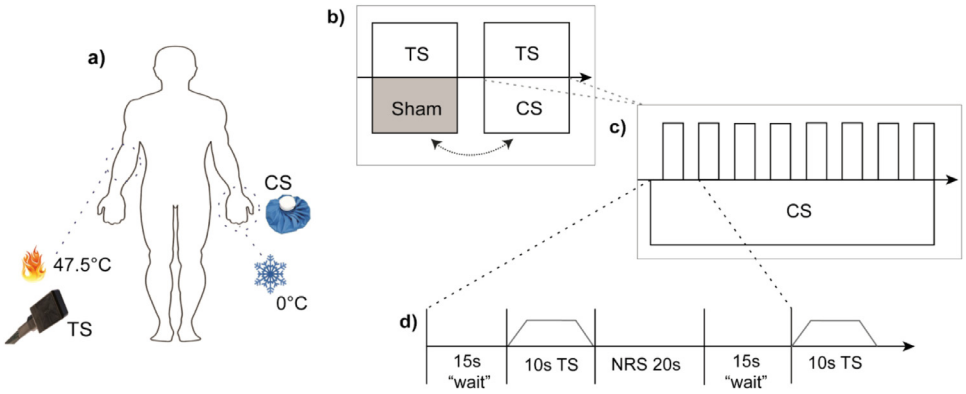

Fig. 1. CPM paradigm
Experimental design of the CPM paradigm performed within the MRI scanner. (**a)** Parallel CPM paradigm was performed with thermal stimuli at the volar forearm and hand. A thermode ramping up to 47.5 °C acted as the TS and two ice bags at around 0 °C on the contralateral hand acted as the CS. (**b)** Individuals underwent two CPM conditions that were randomised. One condition included the application of the genuine CS whilst the other involved the application of two water-filled bags (~32 °C) that acted as the sham CS. (**c,d)** Each condition consisted of eight TS applied to the dominant forearm. Each condition started with a waiting period of 15 s subsequently followed by the TS, which lasted a total time span of 10 s. After each TS, there was a 20-s period during which both TS and CS were rated on an NRS. Therefore, the inter-stimulus interval was 35 s.

2.5. Data analyses

2.5.1. CPM psychophysics

The CPM effect for each subject was calculated as the difference of perceived pain between the TS-CPM and TS-Sham conditions. To this end, the averaged pain ratings of the eight TS during the TS-Sham condition was subtracted from the averaged pain ratings of the eight TS during TS-CPM condition. This provides an overall CPM effect score for each subject: negative numbers represent an inhibitory pain modulation, positive numbers represent a facilitatory pain modulation and a zero represents no effect as previously recommended by Yarnitsky et al. (2015). Individual CPM effect scores were used in the neuroimaging analysis to investigate brain correlates of CPM effect. Furthermore, based on the individual CPM effect scores, subjects were delineated into three subgroups: inhibitor(s), facilitator(s) and non-responder(s) for further analysis (see below).

Statistical analyses were performed with the Statistical Package for the Social Sciences (SPSS) version 24. Histograms, Q-Q plots and Shapiro-Wilk tests were used to test normality of subjects' characteristics and CPM psychophysical readouts. Non-parametric tests were implemented for variables that failed the normality test. To assess the overall CPM effect, a dependant *t*-test was conducted between the averaged pain ratings of the TS under the sham and conditioning condition (TS-CPM vs TS-Sham). Spearman's analysis was implemented to test correlations between subjects' age, BDI score and PCS score with their CPM effect. After sub-grouping, independent t-tests and chi-square test was implemented to assess differences in demographics between inhibitors and facilitators.

2.5.2. Pre-processing for neuroimaging analysis

Both raw structural T1w images and resting-state functional images were pre-processed using Statistical Parametric Mapping (SPM12) software (Statistical parametric mapping; Wellcome Department of Imaging Neuroscience, London, United Kingdom: (http://www.fil.ion.ucl.ac.uk/spm/) implemented in MATLAB 2017a (The Mathworks, Inc, Natick, MA). Prior to pre-processing steps, structural and functional images of each subject were realigned to the anterior commissure (Montreal Neurological Institute (MNI) coordinates; MNI = 0, 0, 0) using the SPM12 display function.

Structural scans were segmented into grey matter, white matter and cerebrospinal fluid using the New Segment tool in SPM12 (Mechelli et al., 2005). Total intracranial volume was calculated from the overall tissue volumes of segmented grey matter, white matter and cerebrospinal fluid maps. The average characteristics of study subjects' grey matter maps were used to create templates using the diffeomorphic non-linear image registration tool (DARTEL) with default values (Ashburner, 2007). DARTEL was implemented to achieve optimal inter-subject alignment before normalisation. Grey matter volumetric maps were spatially normalised to MNI space using the DARTEL-generated template with the modulation function, and then smoothed with a kernel size of 6 mm full-width at half-maximum to conform the data closer to the Gaussian field model (Ashburner and Friston, 2000). Smoothing also renders the data to be more normally distributed and reduces inter-subject variability (Ashburner and Friston, 2000; Mechelli et al., 2005; Whitwell, 2009). Smoothed GMV images were then analysed in SPM12.

Functional images were pre-processed in the following steps: Realignment (head motion correction), centring, slice-timing correction (ascending), outlier detection and outlier scrubbing (using ARtifact detection Tools) during the denoising step (Power et al., 2012, 2013), MNI normalisation and smoothing with 6 mm Gaussian FWHM. The pre-processing steps generated $2 \times 2 \times 2$ mm^3 resolution images for the analyses. Head motion during the resting-state scan was assessed using three translational and rotational dimensions for each scan. Subjects whose mean head motion during the functional scan exceeded +1.5 mm for translation and/or 1° for rotation were removed from rsFC analyses. During the denoising step, normalisation of voxel-to-voxel connectivity values were performed in addition to linear detrending. Subjects that showed normally distributed data after denoising were included into further analyses.

2.5.3. Voxel-based morphometry analysis

A multiple linear regression model was implemented to investigate associations of CPM effect and GMV in the entire cohort. Age, sex, and total intracranial volume were included as covariates of no interest. A composite of supraspinal regions involved with pain processing and descending pain modulation, e.g. bilateral S1, primary motor cortex (M1), insula, ACC, frontal gyri (orbital, inferior, middle, superior, medial) amygdala, thalamus, (Maldjian et al., 2003) was used as an implicit masque in the analysis. Significance was set at $p<0.05$ cluster-level correction (Slotnick et al., 2003). Significant clusters were extracted to create ROIs with the MARSBAR toolbox (Brett et al., 2002) for seed-to-voxel rsFC analysis. GMV of these regions were also extracted and plotted against CPM effect for visualisation.

2.5.4. Seed-to-voxel resting-state functional connectivity analysis

Resting-state functional MRI data was analysed with the CONN toolbox (CONN 18b; www.nitrc.org/projects/conn)(Whitfield-Gabrieli and Nieto-Castanon, 2012). CONN utilises a component-based noise correction method (CompCor) that increases selectivity, sensitivity and allows a higher degree of inter-scan reliability (Behzadi et al., 2007). A band-pass filter (0.01–0.1 Hz) was applied removing linear drift artefacts and high-frequency noise. CONN also accounts for outlier data points and movement time courses as nuisance regressors. The six motion parameters, WM and CSF were included as regressors of no interest, thereby

Table 1
Summary of subjects' characteristics.

Characteristics	Overall (n = 40)	Inhibitors (n = 29)	Facilitators (n = 10)
Demographics			
Age (years)	38 (18 – 74)	37 (18 – 70)	48 (35 – 74)
Sex (F / M)	13 / 27	10 / 19	3 / 7
Handedness (R / L)	38 / 2	28 / 1	9 / 1
Questionnaires			
PCS (0 - 52)	9 (0 – 23)	9 (0 – 23)	10 (0 – 20)
BDI (0 - 63)	2 (0 – 22)	2 (0 – 22)	1 (0 – 4)
Thermal thresholds			
WDT (°C)	36.0 ± 1.5	36.0 ± 1.6	36.2 ± 1.6
HPT (°C)	44.3 ± 2.5	44.5 ± 2.6	44.1 ± 2.7
Pain ratings of noxious stimuli			
Conditioning stimulus (Avg. NRS)	5.5 ± 2.0	5.5 ± 2.1	5.5 ± 2.2
Test stimulus under sham (Avg. NRS)	4.4 ± 1.7	4.5 ± 1.6	4.0 ± 2.2
Test stimulus under CPM (Avg. NRS)	3.8 ± 1.9	3.4 ± 1.7	4.9 ± 2.1
CPM effect			
Test stimulus under CPM (Avg. NRS) – Test stimulus under sham (Avg. NRS)	***−0.57 ± 1.15****	***−1.1 ± 0.8****	***+0.9 ± 0.7****

Data is presented as mean (± standard deviation) or median (range) where appropriate. *Abbreviations:* Avg. – Average; BDI – Beck Depression Inventory; CPM Conditioned Pain Modulation; F – Female; HPT – Heat Pain Threshold; L – Left; M – Male; NRS – Numeric Rating Scale; PCS – Pain Catastrophizing Scale; R – Right; WDT – Warm Detection Threshold; °C – Celsius. PCS scores exceeding 30 indicate clinically relevant levels of catastrophizing. BDI scores between 0 and 13: minimal depression, 14–19: mild depression, 20–28: moderate depression, 29–63: severe depression. *significant difference between test stimulus under CPM and test stimulus under sham at p<0.05.

reducing noise and signal unlikely to reflect neuronal activity related to functional connectivity.

Firstly, multiple linear regression models were implemented to investigate associations of CPM effect and rsFC in the whole subject cohort. Secondly, to test between-group differences in the relationship between CPM effect and seed-to-voxel rsFC a one-way ANCOVA covariate interaction was implemented (Whitfield-Gabrieli and Nieto-Castanon, 2012). Here, seed rsFC values were the dependant variable, and group-by-CPM interactions were the independent variables to compare regressions of CPM effect and rsFC between HC subgroups (inhibitors (n = 29) and facilitators (n = 10) only).

For all analyses, clusters identified in the VBM analysis were used as ROIs for seed-to-voxel analysis and *a priori* ROIs involved with descending pain modulation, e.g. subgenual ACC, amygdala and vlPAG was implemented in the seed-to-voxel analysis. ROIs of the subgenual ACC (Palomero-Gallagher et al., 2015) and amygdala (Amunts et al., 2005) were created in the SPM anatomy toolbox (Eickhoff et al., 2005). ROIs of the left and right vlPAG were defined according to Ezra et al. (2015), Faull and Pattinson (2017). Age and sex were included as covariates of no interest and significant results are reported at p<0.05 cluster-level correction (Whitfield-Gabrieli and Nieto-Castanon, 2012). For visualisation, CPM effects were plotted as a z-score against the rsFC strength (Fisher transformed correlation coefficients) between ROIs showing significant associations. Pearson's r values are reported for visualisation only.

3. Results

3.1. Subject demographics

Two subjects were excluded due to the TS being perceived as too painful during the familiarization. Thus, forty healthy subjects were included in the analysis and their characteristics are summarised in Table 1. No subject exceeded the clinical cut-off values for PCS and BDI. A total PCS score of ≥ 30 represents clinically relevant level of catastrophizing (Sullivan et al., 1995) A BDI score higher than ≥29 indicates severe depression (Dozois et al., 1998). There were no differences in age (p = 0.053), sex (p = 0.460), WDT (p = 0.773) and HPT (p = 0.729) between inhibitors and facilitators. Characteristics of these subgroups are summarised in Table 1.

3.2. CPM psychophysics

All subjects determined the sham condition as non-noxious and the TS and CS as a noxious stimuli, averaged pain ratings of the TS and CS, are summarised in Table 1. In the whole cohort, averaged pain rating of TS-CPM was significantly lower than TS-Sham (p = 0.003) (Fig. 2a). The CPM effect in healthy controls is summarised in Table 1 and the range of individual CPM effects is depicted in Fig. 2b. No correlations were observed between CPM effect and age (p = 0.075, r = 0.284), BDI (p = 0.158, rs=−0.231), PCS (p = 0.533, rs=−0.103) or the rating of the CS (p = 0.211, r=−0.202).

3.3. GMV of pain-related regions and its relation with CPM effect

Significant associations between clusters of GMV and CPM effect were observed (all p<0.05 cluster-level corrected) (Table 2, Figs. 3,4). Greater pain inhibition was associated with higher GMV of the left superior frontal gyrus (SFG) (MNI co-ordinates =−19, 9, 66) (T = 5.25), left inferior frontal gyrus (IFG) near the orbital region (MNI co-ordinates = −49, −5, 45) (T = 3.64) but lower GMV of the right middle frontal gyrus (MFG) (MNI co-ordinates = 19, 8, 67) (T = 4.52).

3.4. rsFC of brain regions and its relation with CPM effect

Significant negative and positive associations between CPM effect and rsFC were observed (Table 3, Figs. 4,5) in the seed-to-voxel analyses. With the cluster of right MFG (identified in the VBM analysis) as the seed region, significant positive associations were observed between CPM effect and rsFC of the right MFG and left S1 (T = 5.71) (p < 0.05 cluster-level corrected). No associations were observed with the left SFG and IFG used as the seed (p > 0.05 cluster-level correction).

A priori ROIs showed significant associations with CPM effect (Table 3). With the left amygdala as a seed, significant positive associations were observed between CPM effect and rsFC to the right posterior insular cortex (T = 5.64) (p < 0.05 cluster-level corrected) (Fig. 5). With

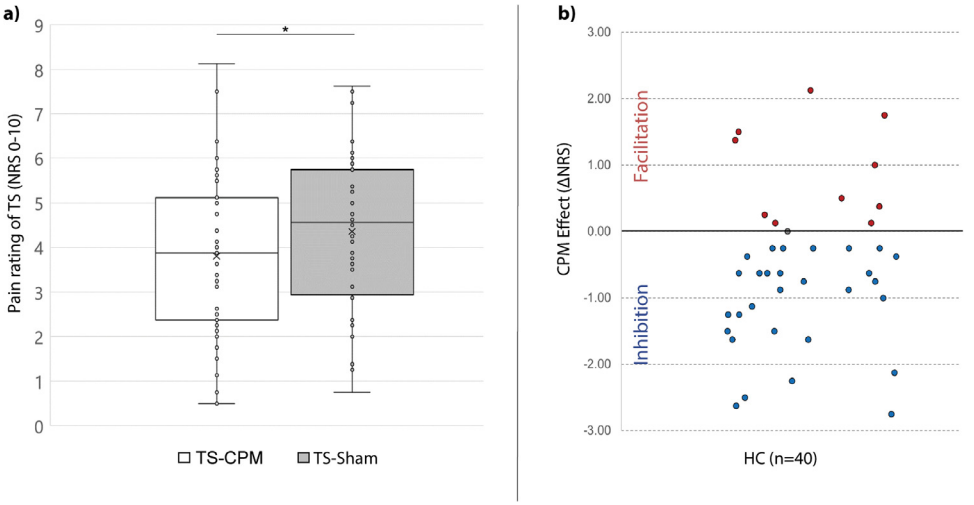

Fig. 2. CPM effect in healthy subjects.
(a) Box plots of averaged pain rating for TS within each condition, i.e., CPM and sham. (b) Scatter plot of individual's CPM effect. Positive numbers describe a facilitatory CPM effect, whilst negative numbers describe an inhibitory CPM effect. Zero describes no CPM effect. *Abbreviations*: CPM – Conditioned Pain Modulation; NRS – Numeric Rating Scale; TS-CPM – Test stimulus during conditioned pain modulation; TS-Sham – Test stimulus during sham condition.

Table 2
Brain regions showing associations of GMV with CPM effect.

GMV and CPM effect in HC (n = 40)	Brain region	MNI co-ordinates (x, y, z)	T-value	Cluster size (kE)
Negative association between GMV and CPM effect	L SFG	−19, 9, 66	5.25	195
	L IFG / OFG	−49, −5, 45	3.64	147
Positive association between GMV and CPM effect	R MFG	19, 8, 67	4.52	160

Associations between GMV of frontal regions and CPM effect in healthy subjects observed in multiple linear regression models. (p<0.05 cluster-level correction). *Abbreviations:* CPM – Conditioned Pain Modulation, GMV – Grey Matter Volume, IFG – Inferior Frontal Gyrus, L – Left, MFG – Middle Frontal Gyrus, MNI – Montreal Neurological Institute, OFG – Orbital Frontal Gyrus, SFG – Superior Frontal Gyrus,.

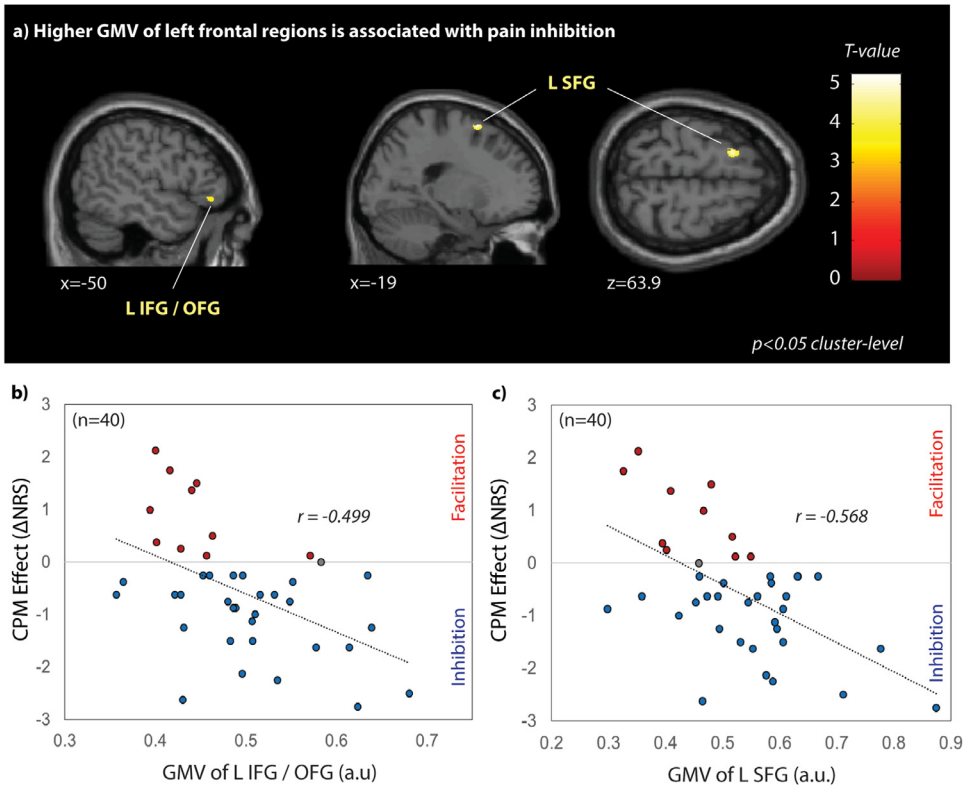

Fig. 3. Pain inhibition in healthy subjects is associated with higher GMV of the left frontal cortex
Overview of negative associations between GMV and CPM effect. (a) Multiple linear regression models showing negative associations between left frontal regions and CPM effect. Healthy subjects with greater pain inhibition during CPM show higher GMV of the left frontal regions (p < 0.05 cluster-level correction), (b,c) Scatter plot representation of CPM effect and GMV of left frontal regions. CPM effect is described as negative and positive numbers, which indicate pain inhibition and facilitation, respectively. GMV are depicted as arbitrary units. Pearson's r values are provided for visualisation only. *Abbreviations*: CPM – Conditioned Pain Modulation, GMV – Grey Matter Volume, IFG – Inferior Frontal Gyrus, L – Left, NRS – Numeric Rating Scale, OFG – Orbital Frontal Gyrus, SFG – Superior Frontal Gyrus.

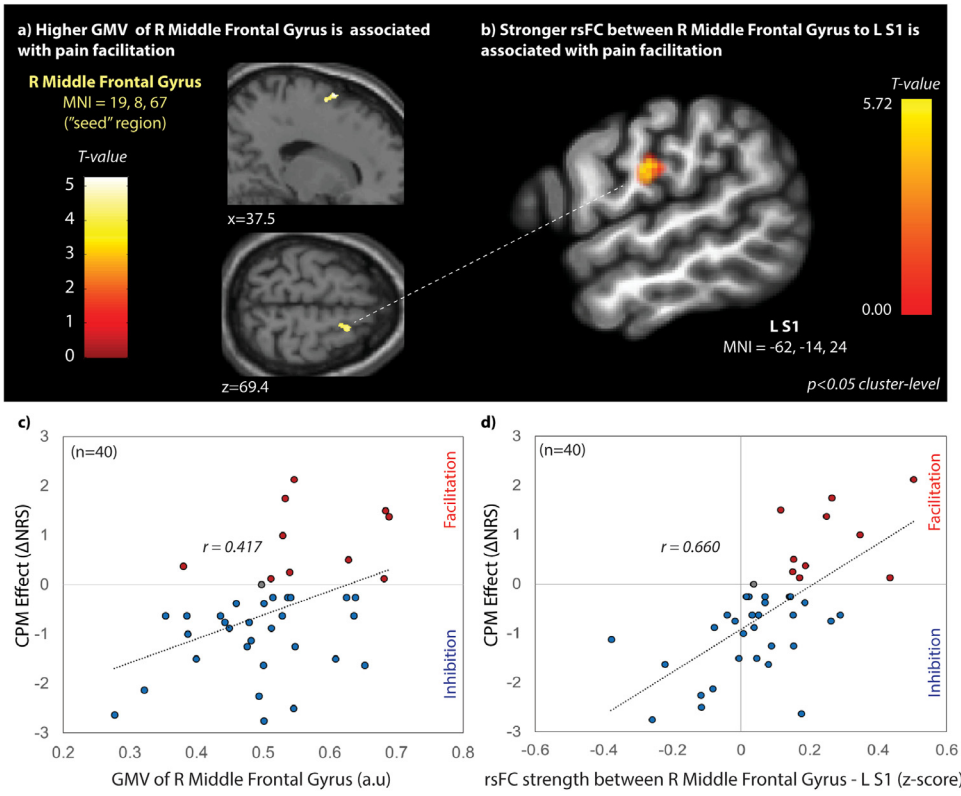

Fig. 4. Pain facilitation in healthy subjects is associated with higher GMV of the right frontal cortex and stronger rsFC to the left somatosensory cortex
(a) Multiple linear regression model showing positive association between GMV of the right middle frontal gyrus and CPM effect. (b) Scatter plot representation of GMV and CPM effect. GMV is depicted in arbitrary units. (c) Using the middle frontal gyrus cluster identified in a) as a "seed", a positive association between CPM effect and rsFC to the left S1 was observed. (d) Scatter plot representation of rsFC between right middle frontal gyrus and left S1 and CPM effect. rsFC strength is depicted as a z-score (Fisher transformed correlation coefficients). CPM effect are described as negative and positive numbers which indicate pain inhibition and facilitation, respectively. *Abbreviations*: CPM – Conditioned Pain Modulation, GMV – Grey Matter Volume, L – Left, MNI – Montreal Neurological Institute, NRS – Numeric Rating Scale, R – Right, rsFC – resting-state Functional Connectivity, S1 – primary somatosensory cortex.

Table 3
Brain regions showing associations with rsFC and CPM effect.

rsFC and CPM effect in HC (n = 40)	Seed-to-voxel	MNI co-ordinates (x, y, z)	T-value	Cluster size (kE)
Positive associations between rsFC and CPM effect	R MFG* - L S1	−62, −14, 24	5.71	199
	L Amygdala – R PIC	28, −30, 10	6.62	143
Negative associations between rsFC and CPM effect	R vlPAG – L M1	−60, 8, 28	−5.17	45
	L vlPAG – L MFG	−40, 36, 40	−4.54	39

Associations between rsFC and CPM effect identified in seed-to-voxel analyses. Positive associations indicate stronger rsFC is related to pain facilitation. Negative associations indicate stronger rsFC is related to pain inhibition. Regions involved with descending pain modulation and clusters (*) observed in VBM analysis (MNI co-ordinates = 19, 8, 67) were used as "seed" regions. *Abbreviations:* CPM – Conditioned Pain Modulation, L – Left, M1 – primary motor cortex, MFG – Middle Frontal Gyrus, MNI – Montreal Neurological Institute, PIC – Posterior Insular Cortex, R – Right, rsFC – resting-state Functional Connectivity, S1 – primary somatosensory cortex. vlPAG – ventrolateral periaqueductal grey.

the right and left vlPAG as the seed, significant negative associations were observed with small clusters of the left motor cortex (T=−4.76) (Fig. 5) and left MFG, respectively (T=−4.54) ($p < 0.05$ cluster-level correction) (Table 3). No associations were observed when the subgenual ACC (left or right) were used as seed regions ($p > 0.05$ cluster-level corrected).

4. Discussion

This is the first study to reveal a relationship between brain structure, rsFC and the efficiency of CPM in healthy subjects. Whilst greater pain inhibition was related to higher volume of the left frontal gyri and stronger rsFC between descending pain modulatory areas, e.g. vlPAG and M1, pain facilitation was related to higher volume of the right MFG, accompanied by stronger rsFC with S1, alongside stronger rsFC between regions involved with the lateral and medial pain systems.

4.1. Neural correlates of CPM efficiency in healthy subjects

CPM can produce a variety of modulatory effects in healthy subjects, ranging from pain inhibition to facilitation (Potvin and Marchand, 2016; Schliessbach et al., 2019). A range of factors may contribute to the variability of CPM efficiency including optimism and pain catastrophising (Goodin et al., 2013), expectation (Bjørkedal and Flaten, 2012), sex (Granot et al., 2008; Skovbjerg et al., 2017) and amounts of brain activity and functional connectivity during CPM (Piché et al., 2009; Sprenger et al., 2011; Bogdanov et al., 2015; Youssef et al., 2016a, 2016b). Beyond CPM studies looking at the modulation of psychophysiological readouts, this study addressed the involvement of brain areas by means of structural (GMV) and functional (rsFC) correlates.

To date, there are limited studies that explored the structural correlates of CPM in healthy subjects (Piché et al., 2013; Coppieters et al., 2018). Our findings were aligned with one study observing that weaker pain inhibition was related to higher volume of the right frontal cortex (Piché et al., 2013) and extend current literature by identifying a relationship between GMV, and rsFC, of the frontal areas and pain modulation. We could show that greater pain inhibition was related to higher GMV of the left frontal regions, e.g. SFG and IFG (Fig. 3) and stronger rsFC between the vlPAG to the left MFG (Table 3). The prefrontal cortices such as the left dorsolateral prefrontal and ventrolateral cortex, have shown involvement with pain suppression and perception of noxious thermal stimuli (Xie et al., 2004; Freund et al.,

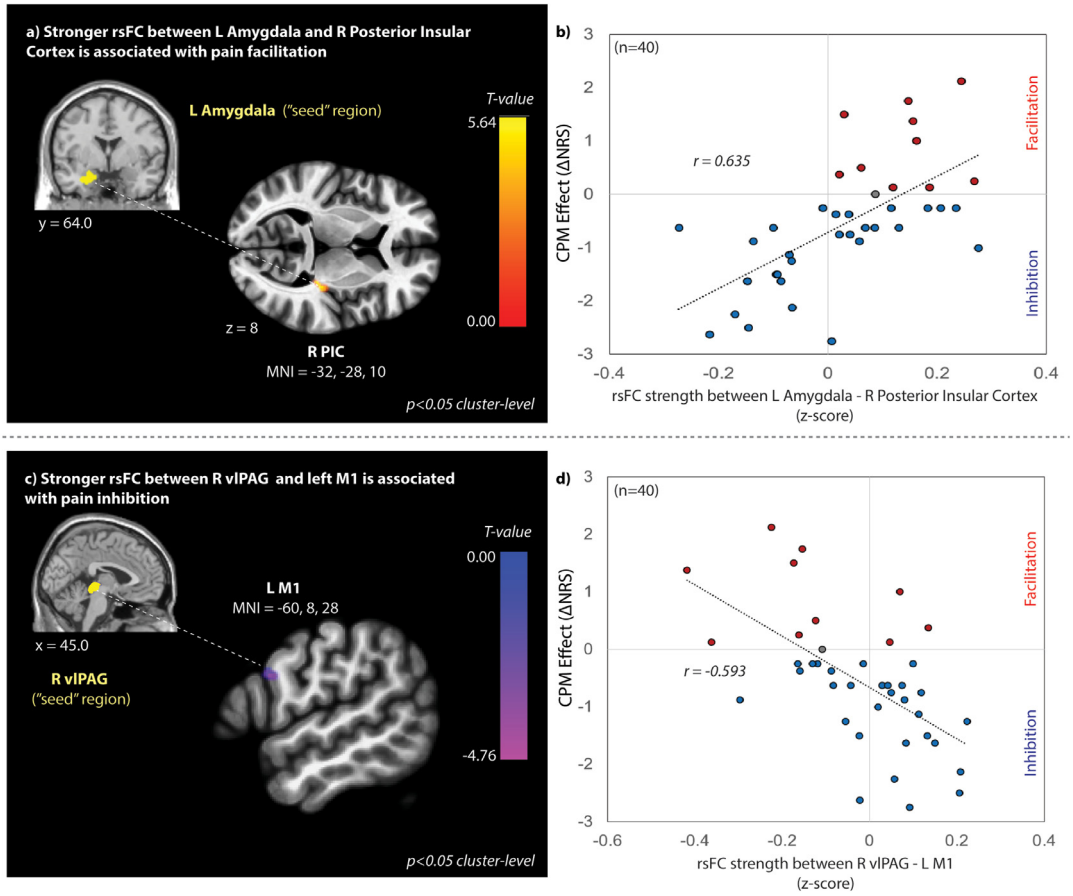

Fig. 5. Pain modulation in healthy subjects is associated with rsFC in regions involved with lateral pain processing and descending pain modulation
Associations between ROIs involved with descending pain modulation and CPM effect. (a) Positive association between CPM effect and rsFC to the right PIC with the left amygdala as a "seed" of interest. (b) Scatter plot representation of pain facilitation and rsFC. (c) Negative association between CPM effect and rsFC to a small cluster of the left M1 with the right vlPAG as a "seed" of interest. (d) Scatter plot representation of pain inhibition and rsFC. The rsFC strength is depicted as a z-score (Fisher transformed correlation coefficients). CPM effects are described as negative and positive numbers, which indicate pain inhibition and facilitation, respectively. *Abbreviations*: CPM – Conditioned Pain Modulation, L – Left, M1 – primary motor cortex, MNI – Montreal Neurological Institute, NRS – Numeric Rating Scale, PIC – Posterior Insular Cortex, R – Right, rsFC – resting-state Functional Connectivity, vlPAG – ventrolateral periaqueductal grey.

2009), and are structurally and functionally altered in acute and chronic pain (Seminowicz and Moayedi, 2017; Ong et al., 2019). Moreover, weaker pain inhibition (to facilitation) was related to higher GMV of the right MFG and stronger rsFC of this same region with S1 (Fig. 4). Thus, this study extends current evidence indicating that increased GMV of the right frontal regions is related to weaker pain inhibition in healthy subjects (Piché et al., 2013), and may also be accompanied by stronger rsFC to S1 (Fig. 4), a terminal region involved with the sensory-discriminative aspects of pain (Bushnell et al., 1999; Tracey and Mantyh, 2007; Xie et al., 2009; Quintero, 2013). Therefore, the variability of GMV and rsFC in frontal cortices and regions involved with descending pain modulation, e.g. vlPAG, and the lateral pain system, e.g. S1, may be related to pain inhibition and facilitation (Table 3, Fig. 5), respectively in healthy subjects. We also observed a relationship between weaker pain inhibition and stronger rsFC between the left amygdala and right PIC (Fig. 5). The left amygdala is involved with the affective components of pain (Thompson and Neugebauer, 2017) and animal studies suggests that the left amygdala may be involved in anti-nociception (Thompson and Neugebauer, 2017) and the posterior insula integrates sensory, nociceptive and affective functions (Starr et al., 2009; Stephani et al., 2011; Segerdahl et al., 2015) which may be reciprocated with amygdala connections (Mufson et al., 1981; Berret et al., 2019). Hence, stronger rsFC in regions involved with the lateral, e.g. S1, posterior insula, and medial, e.g. amygdala, pain systems could be influencing weaker pain inhibitory functions. Current studies have shown that greater pain inhibition is associated with stronger rsFC of the vlPAG (to the medulla) (Harper et al., 2018), and between prefrontal and cingulate cortices (Argaman et al., 2020) in healthy subjects. This study extends evidence by observing that greater pain inhibition is also related to stronger rsFC between the vlPAG and M1 (Fig. 5). Whilst the vlPAG remains an essential site for descending pain modulation (Ossipov et al., 2010, 2014), a recent animal study has reinforced the motor cortex in descending pain control which is orchestrated with the neuronal activity of brainstem regions (Lopes et al., 2019). Further, motor cortex stimulation is a developing method of chronic pain attenuation (Mo et al., 2019), and has been shown to activate supraspinal regions involved with pain processing including the vlPAG, limbic regions and cingulate cortices (Peyron et al., 1995, 2007; García-Larrea et al., 1999; Garcia-Larrea and Peyron, 2007). Thus, stronger connectivity between the motor cortex and brainstem regions, e.g. vlPAG, might underly stronger pain inhibition.

Overall, this study provides further lines of evidence that underlying differences in brain structure and function of distinctive pain processing regions, may contribute to the variability of individual CPM efficiency in healthy subjects. Previous task-related fMRI studies have identified different neural processing in healthy subjects showing pain inhibition or not during CPM, e.g. decreased or increased activation of pain processing areas, e.g. insula, alongside, heightened activity and functional

connectivity of descending pain modulatory regions, e.g. orbitofrontal cortex, cingulate cortex, vlPAG and lower brainstem regions (Song et al., 2006; Piché et al., 2009; Sprenger et al., 2011; Moont et al., 2012; Nahman-Averbuch et al., 2014; Bogdanov et al., 2015; Youssef et al., 2016a, 2016b; Kisler et al., 2018). As a lack of pain inhibition may be a normal finding in healthy subjects (Schliessbach et al., 2019) and CPM effect was not related to psychological factors, i.e., BDI and PCS, accumulating evidence suggests that underlying differences in neural correlates may account for the variability in individual CPM efficiency.

4.2. CPM and neuroimaging in chronic pain conditions

Investigating the variability of CPM efficiency have shown potential use for determining individuals likely to develop chronic post-operative pain. Deficient CPM before knee arthroplasty was associated with less pain relief six months after surgery, indicating that subjects with dysfunctional pain modulatory controls may be at risk of developing chronic pain post-operatively (Yarnitsky et al., 2008). Furthermore, efficient pain inhibition predicted a lower risk of chronic pain development (Yarnitsky et al., 2008) which has been replicated in other studies (Kosek and Ordeberg, 2000; Graven-Nielsen et al., 2012). Various reviews have discussed CPM regarding its reliability, variability, application in chronic pain conditions, and in general standardised protocols are needed in this field of research (Yarnitsky, 2010, 2015; Lewis et al., 2012; Staud, 2012; Ossipov et al., 2014; Nir and Yarnitsky, 2015; Kennedy et al., 2016; Damien et al., 2018; Fernandes et al., 2019; Petersen et al., 2019). However, recent studies have shown promise by combining CPM with neuroimaging readouts to investigate the neural correlates of endogenous pain modulation in chronic pain. Weaker pain inhibition during CPM has been related to higher cortical thickness of the right lateral orbitofrontal cortex in patients with irritable bowel syndrome (Piché et al., 2013), lower microstructural integrity of the precuneus in chronic neck pain (Coppieters et al., 2018), and stronger rsFC between the vlPAG and RVM in fibromyalgia (Harper et al., 2018). Interestingly, although pain inhibition was observed in migraineurs, the relationship between CPM efficiency and rsFC of the default mode network was altered compared to healthy subjects (Argaman et al., 2020).

Overall, though reviews indicate that standardised protocols of CPM are needed, growing evidence shows that the combined use of neuroimaging may benefit future studies investigating the neural correlates of CPM efficiency and its dysfunction in pain conditions.

4.3. Methodological considerations

This study consists of some limitations. Firstly, the CPM paradigm was adapted and performed within the constraints of an MRI scanner and may not adhere to the recommendations of CPM testing, e.g. only the use of one stimulus modality was used in this study (Yarnitsky et al., 2015). Secondly, the MRI analysis was not optimised for lower brainstem regions and indeed, optimising these parameters allows more precise examinations of lower brainstem regions (e.g. pons and medulla) activity in CPM (Youssef et al., 2016b). Future rsFC studies may benefit by optimising parameters solely on the brainstem regions. Finally, the acquisition time of the resting-state fMRI is five minutes, and although this duration is able to acquire stable estimates of intrinsic connectivity networks (Fox et al., 2005; Van Dijk et al., 2010), longer acquisition times (e.g. up to 13 min) may increase the reliability of functional connectivity (Birn et al., 2013).

5. Conclusion

The findings of this study extend accumulating evidence suggesting that CPM efficiency in healthy subjects is associated with underlying differences in brain structure and function. Specifically, stronger pain inhibition and facilitation may be related to higher volume and stronger connectivity in key regions involved with descending pain modulation, i.e., vlPAG and M1, and pain processing, i.e., amygdala, S1, posterior insula, respectively. In general, studies that investigate the relationship between underlying brain structure, rsFC and CPM are limited and future studies with larger cohorts are needed to corroborate these findings. However, combining neuroimaging and CPM may provide a suitable avenue to identify the neural correlates of endogenous pain modulation to provide a framework for deepening our understanding of its pathophysiology in chronic pain cohorts.

Declaration of Competing Interest

The authors declare no conflict of interest.

Acknowledgements

This project is funded by the Swiss National Science Foundation (320030_169250) and the Clinical Research Priority Program of the University of Zurich (CRPP Pain). The authors also thank all subjects who participated in this study and Jessica Archibald MSc (University of British Columbia) for programming the initial script for the numeric rating scale for data collection.

Subject consent statement

All subjects provided written informed consent prior to the assessments and were reimbursed for their participation.

Ethics approval

All procedures described in this study were in accordance with the Declaration of Helsinki and have been approved by the local ethics board ‘Kantonale Ethikkommission Zürich, KEK’ (EK-04/2006, PB_2016–02051, clinicaltrial.gov number: NCT02138344).

Supplementary materials

Supplementary material associated with this article can be found, in the online version, at doi:10.1016/j.neuroimage.2021.118742.

References

Albu, S., et al., 2015. Deficient conditioned pain modulation after spinal cord injury correlates with clinical spontaneous pain measures. Pain 156 (2), 260–272. doi:10.1097/01.j.pain.0000460306.48701.f9.

Amunts, K., et al., 2005. Cytoarchitectonic mapping of the human amygdala, hippocampal region and entorhinal cortex: intersubject variability and probability maps. Anat. Embryol. doi:10.1007/s00429-005-0025-5.

Argaman, Y., et al., 2020. The endogenous analgesia signature in the resting brain of healthy adults and migraineurs. J. Pain doi:10.1016/j.jpain.2019.12.006.

Ashburner, J., 2007. A fast diffeomorphic image registration algorithm. Neuroimage doi:10.1016/j.neuroimage.2007.07.007.

Ashburner, J., Friston, K.J., 2000. Voxel-based morphometry-the methods. Neuroimage 11 (6), 805–821. doi:10.1006/nimg.2000.0582.

Behzadi, Y., et al., 2007. A component based noise correction method (CompCor) for BOLD and perfusion based fMRI. Neuroimage.

Berret, E., et al., 2019. Insular cortex processes aversive somatosensory information and is crucial for threat learning. Science doi:10.1126/science.aaw0474.

Birn, R.M., et al., 2013. The effect of scan length on the reliability of resting-state fMRI connectivity estimates. Neuroimage doi:10.1016/j.neuroimage.2013.05.099.

Bjørkedal, E., Flaten, M.A., 2012. Expectations of increased and decreased pain explain the effect of conditioned pain modulation in females. J. Pain Res. doi:10.2147/JPR.S33559.

Bogdanov, V.B., et al., 2015. Cerebral responses and role of the prefrontal cortex in conditioned pain modulation: an fMRI study in healthy subjects. Behav. Brain Res. doi:10.1016/j.bbr.2014.11.028.

Brett, M., et al., 2002. Region of interest analysis using the MarsBar toolbox for SPM99. In: Proceedings of the 8th International Congress on Functional Mapping of the Human Brain, pp. 2–6. doi:10.1016/S1053-8119(02)90010-8.

Bushnell, M.C., et al., 1999. Pain perception: is there a role for primary somatosensory cortex? Proc. Natl. Acad. Sci. U. S. A. doi:10.1073/pnas.96.14.7705.

Chen, T., et al., 2018. Top-down descending facilitation of spinal sensory excitatory transmission from the anterior cingulate cortex. Nat. Commun. 9 (1). doi:10.1038/s41467-018-04309-2.

Coppieters, I., et al., 2018. Differences in white matter structure and cortical thickness between patients with traumatic and idiopathic chronic neck pain: associations with cognition and pain modulation? Hum. Brain Mapp. doi:10.1002/hbm.23947.

Damien, J., et al., 2018. Pain modulation: from conditioned pain modulation to placebo and nocebo effects in experimental and clinical Pain. Int. Rev. Neurobiol. doi:10.1016/bs.irn.2018.07.024.

Dickenson, A.H., Le Bars, D., Besson, J.M., 1980. Diffuse noxious inhibitory controls (DNIC). Effects on trigeminal nucleus caudalis neurones in the rat. Brain Res. doi:10.1016/0006-8993(80)90921-X.

Van Dijk, K.R.A., et al., 2010. Intrinsic functional connectivity as a tool for human connectomics: theory, properties, and optimization. J. Neurophysiol. doi:10.1152/jn.00783.2009.

Dozois, D.J.A., Dobson, K.S., Ahnberg, J.L., 1998. A psychometric evaluation of the Beck Depression Inventory-II. Psychol. Assess. doi:10.1037/1040-3590.10.2.83.

Edwards, R.R., Fillingim, R.B., Ness, T.J., 2003. Age-related differences in endogenous pain modulation: a comparison of diffuse noxious inhibitory controls in healthy older and younger adults. Pain doi:10.1016/S0304-3959(02)00324-X.

Eickhoff, S.B., et al., 2005. A new SPM toolbox for combining probabilistic cytoarchitectonic maps and functional imaging data. Neuroimage 25 (4), 1325–1335. doi:10.1016/j.neuroimage.2004.12.034.

Ezra, M., et al., 2015. Connectivity-based segmentation of the periaqueductal gray matter in human with brainstem optimized diffusion MRI. Hum. Brain Mapp. doi:10.1002/hbm.22855.

Faull, O.K., Pattinson, K.T.S., 2017. The cortical connectivity of the periaqueductal gray and the conditioned response to the threat of breathlessness. Elife doi:10.7554/eLife.21749.

Fernandes, C., et al., 2019. Conditioned pain modulation as a biomarker of chronic pain: a systematic review of its concurrent validity. Pain doi:10.1097/j.pain.0000000000001664.

Fox, M.D., et al., 2005. The human brain is intrinsically organized into dynamic, anticorrelated functional networks. Proc. Natl. Acad. Sci. U. S. A. doi:10.1073/pnas.0504136102.

Freund, W., et al., 2009. Perception and suppression of thermally induced pain: a fMRI study. Somatosens. Motor Res. doi:10.1080/08990220902738243.

García-Larrea, L., et al., 1999. Electrical stimulation of motor cortex for pain control: a combined PET-scan and electrophysiological study. Pain doi:10.1016/S0304-3959(99)00114-1.

Garcia-Larrea, L., Peyron, R., 2007. Motor cortex stimulation for neuropathic pain: from phenomenology to mechanisms. Neuroimage doi:10.1016/j.neuroimage.2007.05.062.

Goodin, B.R., Glover, T.L., Sotolongo, A., King, C.D., Sibille, K.T., Herbert, M.S., et al., 2013. The association of greater dispositional optimism with less endogenous pain facilitation is indirectly transmitted through lower levels of pain catastrophizing. Pain doi:10.1016/j.jpain.2012.10.007.

Granot, M., et al., 2008. Determinants of endogenous analgesia magnitude in a diffuse noxious inhibitory control (DNIC) paradigm: do conditioning stimulus painfulness, gender and personality variables matter? Pain doi:10.1016/j.pain.2007.06.029.

Graven-Nielsen, T., et al., 2012. Normalization of widespread hyperesthesia and facilitated spatial summation of deep-tissue pain in knee osteoarthritis patients after knee replacement. Arthritis Rheumatol. doi:10.1002/art.34466.

Gruener, H., et al., 2016. Differential pain modulation properties in central neuropathic pain after spinal cord injury. Pain doi:10.1097/j.pain.0000000000000532.

Harper, D.E., et al., 2018. Resting functional connectivity of the periaqueductal gray is associated with normal inhibition and pathological facilitation in conditioned pain modulation. J. Pain doi:10.1016/J.JPAIN.2018.01.001.

Huang, J., et al., 2019. A neuronal circuit for activating descending modulation of neuropathic pain. Nat. Neurosci. doi:10.1038/s41593-019-0481-5.

Kennedy, D.L., et al., 2016. Reliability of conditioned pain modulation: a systematic review. Pain 2410–2419. doi:10.1097/j.pain.0000000000000689.

Kisler, L.B., et al., 2018. Do patients with interictal migraine modulate pain differently from healthy controls? A psychophysical and brain imaging study. Pain doi:10.1097/j.pain.0000000000001380.

Kosek, E., Ordeberg, G., 2000. Lack of pressure pain modulation by heterotopic noxious conditioning stimulation in patients with painful osteoarthritis before, but not following, surgical pain relief. Pain doi:10.1016/S0304-3959(00)00310-9.

Le Bars, D., et al., 1992. Diffuse noxious inhibitory controls (DNIC) in animals and in man. Patologicheskaia fiziologiia i èksperimental'naia terapiia doi:10.1136/aim.9.2.47.

Le Bars, D., Chitour, D., Clot, A.M, 1981. The encoding of thermal stimuli by diffuse noxious inhibitory controls (DNIC). Brain Res. 230 (1–2), 394–399. doi:10.1016/0006-8993(81)90422-4.

Le Bars, D., Dickenson, A.H., Besson, J.M, 1979a. Diffuse noxious inhibitory controls (DNIC). I. Effects on dorsal horn convergent neurones in the rat. Pain doi:10.1016/0304-3959(79)90049-6.

Le Bars, D., Le Dickenson, A.H., Besson, J.marie, 1979b. Diffuse noxious inhibitory controls (DNIC). II. Lack of effect on non-convergent neurones, supraspinal involvement and theoretical implications. Pain doi:10.1016/0304-3959(79)90050-2.

Lewis, G.N., et al., 2012. Reliability of the conditioned pain modulation paradigm to assess endogenous inhibitory pain pathways. Pain Res. Manag. 17 (2), 98–102. doi:10.1155/2012/610561.

Liu, Y., et al., 2018. Touch and tactile neuropathic pain sensitivity are set by corticospinal projections. Nature doi:10.1038/s41586-018-0515-2.

Lopes, P.S.S., et al., 2019. Motor cortex and pain control: exploring the descending relay analgesic pathways and spinal nociceptive neurons in healthy conscious rats. Behav. Brain Funct. doi:10.1186/s12993-019-0156-0.

Maldjian, J.A., et al., 2003. An automated method for neuroanatomic and cytoarchitectonic atlas-based interrogation of fMRI data sets. Neuroimage 19 (3), 1233–1239. doi:10.1016/S1053-8119(03)00169-1.

McPhee, M.E., Vaegter, H.B., Graven-Nielsen, T., 2019. Alterations in pro-nociceptive and anti-nociceptive mechanisms in patients with low back pain. Pain doi:10.1097/j.pain.0000000000001737.

Mechelli, A., et al., 2005. Voxel-based morphometry of the human brain: methods and applications. Curr. Med. 1 (2), 105–113. doi:10.2174/1573405054038726.

Mo, J.J., et al., 2019. Motor cortex stimulation: a systematic literature-based analysis of effectiveness and case series experience. BMC Neurol. doi:10.1186/s12883-019-1273-y.

Moont, R., et al., 2012. Temporal changes in cortical activation during distraction from pain: a comparative LORETA study with conditioned pain modulation. Brain Res. doi:10.1016/j.brainres.2011.11.056.

Mufson, E.J., Mesulam, M.M., Pandya, D.N., 1981. Insular interconnections with the amygdala in the rhesus monkey. Neuroscience doi:10.1016/0306-4522(81)90184-6.

Nahman-Averbuch, H., et al., 2014. Distinct brain mechanisms support spatial vs temporal filtering of nociceptive information. Pain doi:10.1016/j.pain.2014.07.008.

Nir, R.-R., Yarnitsky, D, 2015. Conditioned pain modulation. Curr. Opin. Support. Palliat. Care 9 (2), 131–137. doi:10.1097/SPC.0000000000000126.

O'Brien, A.T., et al., 2018. Defective endogenous pain modulation in fibromyalgia: a meta-analysis of temporal summation and conditioned pain modulation paradigms. J. Pain doi:10.1016/j.jpain.2018.01.010.

Ong, W.Y., Stohler, C.S., Herr, D.R., 2019. Role of the prefrontal cortex in pain processing. Mol. Neurobiol. doi:10.1007/s12035-018-1130-9.

Ossipov, M.H., Dussor, G.O., Porreca, F., 2010. Central modulation of pain. J. Clin. Investig. 3779–3787. doi:10.1172/JCI43766.

Ossipov, M.H., Morimura, K., Porreca, F., 2014. Descending pain modulation and chronification of pain. Curr. Opin. Support. Palliat. Care 143–151. doi:10.1097/SPC.0000000000000055.

Palomero-Gallagher, N., et al., 2015. Functional organization of human subgenual cortical areas: relationship between architectonical segregation and connectional heterogeneity. Neuroimage doi:10.1016/j.neuroimage.2015.04.053.

Petersen, K.K., et al., 2019. Assessment of conditioned pain modulation in healthy participants and patients with chronic pain: manifestations and implications for pain progression. Curr. Opin. Support. Palliat. Care doi:10.1097/SPC.0000000000000419.

Peyron, R., et al., 1995. Electrical stimulation of precentral cortical area in the treatment of central pain: electrophysiological and PET study. Pain doi:10.1016/0304-3959(94)00211-V.

Peyron, R., et al., 2007. Motor cortex stimulation in neuropathic pain. Correlations between analgesic effect and hemodynamic changes in the brain. A PET study. Neuroimage doi:10.1016/j.neuroimage.2006.08.037.

Piché, M., et al., 2013. Thicker posterior insula is associated with disease duration in women with irritable bowel syndrome (IBS) whereas thicker orbitofrontal cortex predicts reduced pain inhibition in both IBS patients and controls. J. Pain doi:10.1016/j.jpain.2013.05.009.

Piché, M., Arsenault, M., Rainville, P., 2009. Cerebral and cerebrospinal processes underlying counterirritation analgesia. J. Neurosci. doi:10.1523/JNEUROSCI.2341-09.2009.

Potvin, S., Marchand, S., 2016. Pain facilitation and pain inhibition during conditioned pain modulation in fibromyalgia and in healthy controls. Pain doi:10.1097/j.pain.0000000000000573.

Power, J.D., et al., 2012. Spurious but systematic correlations in functional connectivity MRI networks arise from subject motion. Neuroimage 59 (3), 2142–2154. doi:10.1016/j.neuroimage.2011.10.018.

Power, J.D., et al., 2013. Steps toward optimizing motion artifact removal in functional connectivity MRI; a reply to Carp. Neuroimage doi:10.1016/j.neuroimage.2012.03.017.

Quintero, G.C., 2013. Advances in cortical modulation of pain. J Pain Res doi:10.2147/JPR.S45958.

Rolke, R., et al., 2006. Quantitative sensory testing: a comprehensive protocol for clinical trials. Eur. J. Pain doi:10.1016/j.ejpain.2005.02.003.

Schliessbach, J., et al., 2019. Reference values of conditioned pain modulation. Scand. J. Pain doi:10.1515/sjpain-2018-0356.

Segerdahl, A.R., et al., 2015. The dorsal posterior insula subserves a fundamental role in human pain. Nat. Neurosci. 18 (4), 499–500. doi:10.1038/nn.3969.

Seminowicz, D.A., Moayedi, M., 2017. The dorsolateral prefrontal cortex in acute and chronic pain. J. Pain doi:10.1016/j.jpain.2017.03.008.

Slotnick, S.D., et al., 2003. Distinct prefrontal cortex activity associated with item memory and source memory for visual shapes. Cognit. Brain Res. 17 (1), 75–82. doi:10.1016/S0926-6410(03)00082-X.

Skovbjerg, S., Jørgensen, T., Arendt-Nielsen, L., Ebstrup, J.F., Carstensen, T., Graven-Nielsen, T., 2017. Conditioned pain modulation and pressure pain sensitivity in the adult Danish general population: the DanFunD study. Pain doi:10.1016/j.jpain.2016.10.022.

Song, G.H., et al., 2006. Cortical effects of anticipation and endogenous modulation of visceral pain assessed by functional brain MRI in irritable bowel syndrome patients and healthy controls. Pain doi:10.1016/j.pain.2006.06.017.

Sprenger, C., Bingel, U., Büchel, C., 2011. Treating pain with pain: supraspinal mechanisms of endogenous analgesia elicited by heterotopic noxious conditioning stimulation. Pain doi:10.1016/j.pain.2010.11.018.

Starr, C.J., et al., 2009. Roles of the insular cortex in the modulation of pain: insights from brain lesions. J. Neurosci. doi:10.1523/JNEUROSCI.5173-08.2009.

Staud, R., 2012. Abnormal endogenous pain modulation is a shared characteristic of many chronic pain conditions. Expert Rev. Neurother. doi:10.1586/ern.12.41.

Stephani, C., et al., 2011. Functional neuroanatomy of the insular lobe. Brain Struct. Funct. 216 (2), 137–149. doi:10.1007/s00429-010-0296-3.

Sullivan, M.J.L., Bishop, S.R., Pivik, J., 1995. The pain catastrophizing scale: development and validation. Psychol. Assess. doi:10.1037/1040-3590.7.4.524.

Whitfield-Gabrieli, S., Nieto-Castanon, A., 2012. Conn: a functional connectivity toolbox for correlated and anticorrelated brain networks. Brain Connect 2 (3), 125–141. doi:10.1089/brain.2012.0073.

Thompson, J.M., Neugebauer, V., 2017. Amygdala Plasticity and Pain. Pain Res. Manag. doi:10.1155/2017/8296501.

Tracey, I., Mantyh, P.W., 2007. The cerebral signature for pain perception and its modulation. Neuron doi:10.1016/j.neuron.2007.07.012.

Vaegter, H.B., et al., 2017. Preoperative hypoalgesia after cold pressor test and aerobic exercise is associated with pain relief 6 months after total knee replacement. Clin. J. Pain doi:10.1097/AJP.0000000000000428.

Villanueva, L., Le Bars, D, 1995. The activation of bulbo-spinal controls by peripheral nociceptive inputs: diffuse noxious inhibitory controls. Biol. Res. 113–125.

Whitwell, J.L., 2009. Voxel-based morphometry: an automated technique for assessing structural changes in the brain. J. Neurosci. doi:10.1523/JNEUROSCI.2160-09.2009.

Xie, Y.F., et al., 2004. 'μ but not δ and κ opioid receptor involvement in ventrolateral orbital cortex opioid-evoked antinociception in formalin test rats. Neuroscience doi:10.1016/j.neuroscience.2004.04.013.

Xie, Y.F., Huo, F.Q., Tang, J.S., 2009. Cerebral cortex modulation of pain. Acta Pharmacol. Sin. doi:10.1038/aps.2008.14.

Yarnitsky, D., et al., 2008. Prediction of chronic post-operative pain: pre-operative DNIC testing identifies patients at risk. Pain 138 (1), 22–28. doi:10.1016/j.pain.2007.10.033.

Yarnitsky, D., 2010. Conditioned pain modulation (the diffuse noxious inhibitory control-like effect): its relevance for acute and chronic pain states. Curr. Opin. Anaesthesiol. 611–615. doi:10.1097/ACO.0b013e32833c348b.

Yarnitsky, D., et al., 2015. Recommendations on practice of conditioned pain modulation (CPM) testing. *Eur. J. Pain* doi:10.1002/ejp.605, United Kingdom.

Yarnitsky, D., 2015. Role of endogenous pain modulation in chronic pain mechanisms and treatment. Pain S24–S31. doi:10.1097/01.j.pain.0000460343.46847.58.

Youssef, A.M., Macefield, V.G., Henderson, L.A., 2016a. Cortical influences on brainstem circuitry responsible for conditioned pain modulation in humans. Hum. Brain Mapp. doi:10.1002/hbm.23199.

Youssef, A.M., Macefield, V.G., Henderson, L.A., 2016b. Pain inhibits pain; human brainstem mechanisms. Neuroimage doi:10.1016/j.neuroimage.2015.08.060.